Beam Delivery Systems

P. Ambatu[3], **D. Angal-Kalinin**[1], *J. Barranco*[4], *G. Blair*[2], *G. Burt*[3], *H. Burkhardt*[4], *B. Dalena*[4], *L. Deacon*[2], *A. Dexter*[3], *H.M. Durand*[4], *J.L. Fernandez Hernando*[1], *L. Gatignon*[4], *F. Jackson*[1], *J. Jones*[1] *E. Marín*[4], *A. Latina*[4], *J. Resta López*[2], *G. Rumolo*[4], *J. Snuverink*[4], *P. Schuler*[5], *D. Schulte*[4], **A. Seryi**[2], **R. Tomás**[4], *V. Vlachoudis*[4], *R. Veness*[4] *and G. Zamudio*[4]
[1]Cockroft Institute, [2]John Adams Institute, [3]Lancaster University, [4]CERN, [5]DESY

3.5 Beam Delivery Systems

3.5.1 Overview

The CLIC Beam Delivery System (BDS) is responsible for transporting the e^+/e^- beams from the exit of the high energy linacs, focusing them to the sizes required to meet the CLIC luminosity goals (σ_x = 45 nm, σ_y = 1 nm in the nominal parameters) and bringing them into collision. In addition, the BDS must perform several critical functions:

1. Measure the linac beam and match it into the final focus.
2. Protect the beamline and detector against mis-steered beams from the main linacs.
3. Remove any large amplitude particles (beam-halo) from the linac to minimize background in the detectors.
4. Measure and monitor the key physics parameters such as energy and polarization.

Functions 2. and 3. are accomplished by the collimators. Therefore the first collimator needs to survive to the impact of any mis-steered CLIC bunch train. This condition requires large beam sizes at the first collimator, hence driving the length of the system. The BDS must provide sufficient instrumentation, diagnostics and feedback systems to achieve these goals. All the CLIC BDS lattices can be found in [1].

3.5.2 Beam parameters

Table 1 shows the key BDS parameters for the nominal configuration at 3 TeV CM.

3.5.3 Subsystems

The main subsystems of the beam delivery starting from the exit of the main linacs are the diagnostics region, the energy and betatron collimation and the final focus. The layout of the beam delivery system is shown in Fig. 1.

There is a single collision point with a 20 mrad crossing angle. The 20 mrad geometry provides space for separated spent beam lines and requires crab cavities to rotate the bunches in the horizontal plane for head-on collisions. There are two detectors in a common IR cavern complex (plus two garage caverns) which alternately occupy the single collision point, in a so-called "push-pull" configuration, see Section 5.10.2.5 for more details.

3.5.3.1 Diagnostics

The initial part of the BDS, from the end of the main linac to the start of the collimation system, is responsible for measuring and correcting the properties of the beam before it enters the Collimation and Final Focus system. The optics and the layout of the diagnostics section is shown in Fig. 2. Starting at the exit of the main linac, the system includes the skew correction section, emittance diagnostic section and beta matching section. The skew correction section contains 4 orthonormal skew quadrupoles which provide complete and independent control of the 4 betatron coupling parameters. This scheme allows correction of any arbitrary linearized coupled beam.

Table 1: Key parameters of the BDS. The range of L*, the distance from the final quadrupole to the IP, corresponds to values considered for different detector and FFS concepts.

Parameter	Units	Value
Length (linac exit to IP distance)/side	m	2750
Maximum Energy/beam	TeV	1.5
Distance from IP to first quad, L*	m	3.5-6
Crossing angle at the IP	mrad	20
Nominal core beam size at IP, σ^*, x/y	nm	45/1
Nominal beam divergence at IP, θ^*, x/y	μrad	7.7/10.3
Nominal beta-function at IP, β^*, x/y	mm	10/0.07
Nominal bunch length, σ_z	μm	44
Nominal disruption parameters, x/y		0.15/8.4
Nominal bunch population, N		3.7×10^9
Beam power in each beam	MW	14
Preferred entrance train to train jitter	σ	< 0.2
Preferred entrance bunch to bunch jitter	σ	< 0.05
Typical nominal collimation aperture, x/y	σ_x/σ_y	15/55
Vacuum pressure level, near/far from IP	nTorr	1000/1

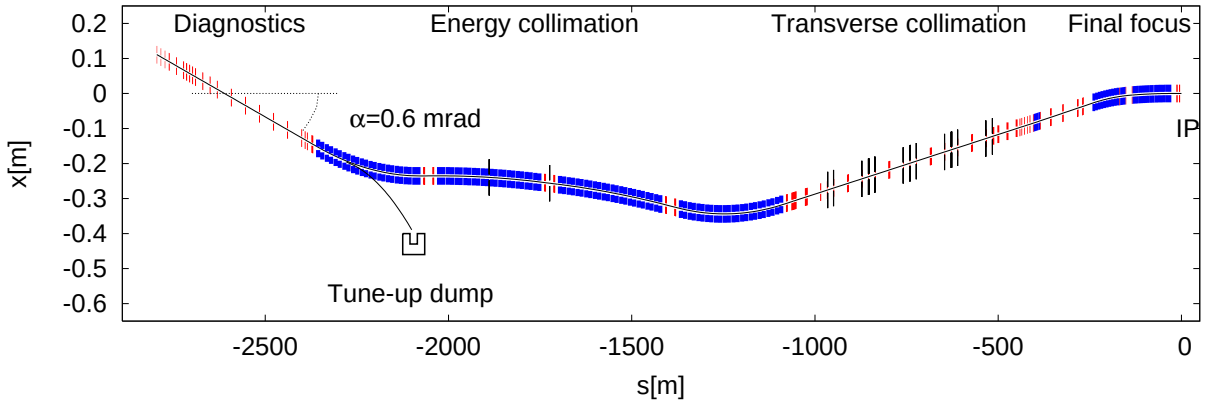

Fig. 1: CLIC 3 TeV layout. Dipoles, quadrupoles and collimators are shown in blue, red and black, respectively. The tune-up dump and its extraction line are also displayed.

The emittance diagnostic section contains 4 laser wires which are capable of measuring horizontal and vertical RMS beam sizes down to 1 μm. The wire scanners are separated by 45° in betatron phase to allow a complete measurement of 2D transverse phase space and determination of the projected horizontal and vertical emittances.

The energy measurement has been designed to minimize the required space due to the tight constraints on the CLIC total length. The deflection of the first dipole in the energy collimation section together with high precision BPM pairs at both sides of the dipole provides the most compact energy measurement. The integrated magnetic field is assumed to have a calibration error of 0.01% and the BPM resolution must be 50 nm or better with a maximum calibration error of 0.1%. This set-up provides a relative energy resolution below 0.1%. Reference trajectories can be regularly established by zeroing

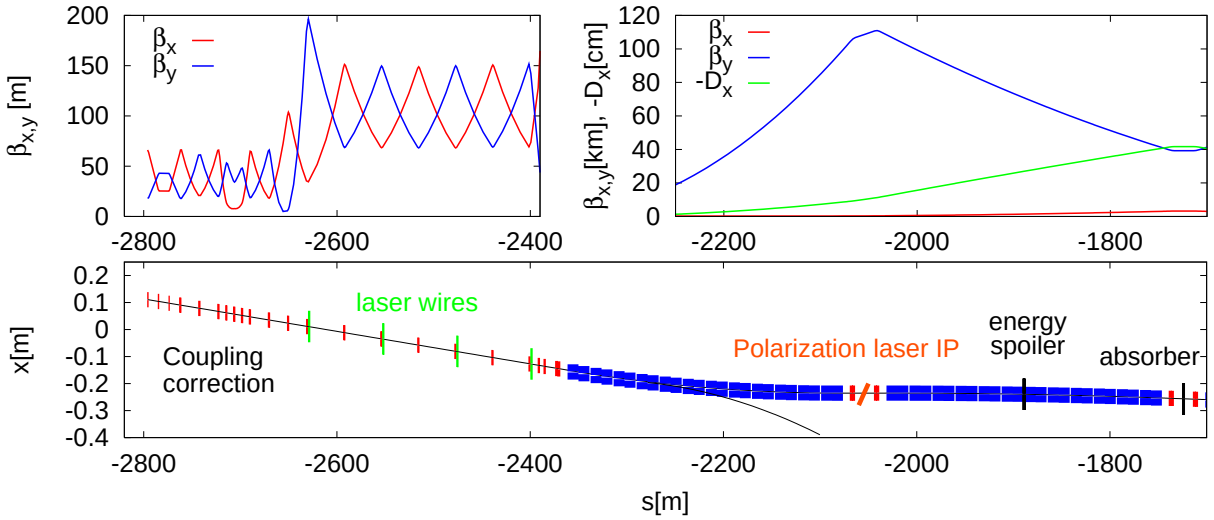

Fig. 2: Optics (top) and layout (bottom) of the CLIC diagnostics and energy collimation sections.

the magnetic field and safely disposing of the beam in the tune-up dump.

The BDS is equipped with a polarization measurement station [2] in the energy collimation section. Figure 2 shows the location of the polarization laser IP. At this location the beam travels parallel to the beam direction at the e^--e^+ IP and there is enough free space for the polarization laser. The back scattered electrons (or positrons) will deviate from the main beam trajectory thanks to the bending dipoles. These lower energy particles can be collected in a detector right before the energy spoiler. Excursions in the order of 100 mm are expected for particles loosing about 95% of the energy. With current existing laser technology the polarization measurement achieves a resolution better than 0.1% if averaging over 60 seconds. The systematic errors of the set-up will be analyzed in the forthcoming technical design phase.

3.5.3.2 Tune-up extraction lines & dumps

During the commissioning of the main linacs the presence of the beam is not desired in the collimation, final focus, or IR areas. An extraction line right before the energy collimation allows to guide the beam to a full-beam power water-filled dump.

3.5.3.3 Collimation

The CLIC collimation section fulfills two critical functions. (1) It protects the down-stream beam line and detector against mis-steered beams from the main linac and (2) removes the beam halo. The most likely scenario for having mis-steered beams in the BDS is the failure of some component of the accelerating RF in the 20 km linac, resulting in a lower beam energy. Therefore placing the energy collimation before the betatron collimation guarantees the most efficient absorption of the errant beams. The energy spoiler is designed to survive the impact of a full bunch train. The spoiler survives medium depth impacts up to 2 mm [3]. However recent simulations show that deep impacts may damage the energy spoiler [4]. This is due to the increase in the collimator length for deeper impacts. A solution would be to consider a hollow collimator. This should be investigated during the technical phase together with failure modes in the LINAC as the deep impacts might turn out improbable or associated to large emittance dilution.

The transverse collimators, made of Ti, are sacrificial or consumable. A collimator absorber is placed downstream the spoiler as shown in Fig. 3 to stop the particles scattered at the spoiler. The full

Table 2: Geometry of the BDS spoilers and absorbers. The radiation lengths for Be and Ti are X_0=0.353 m and X_0=0.036 m, respectively. The material (Ti-Cu) of the transverse spoilers (YSP and XSP) is Ti with a Cu coating.

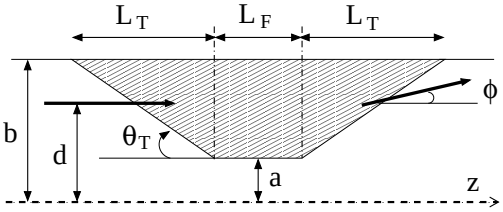

Name	a_x [mm]	a_y [mm]	θ_T [mrad]	L_F [X_0]	L_T [mm]	Mat.
ESP	3.51	8	50	0.05	90	Be
EAB	5.41	8	100	18	27	Ti
the following ×4						
YSP	8	0.1	88	0.2	90	Ti-Cu
XSP	0.12	8	88	0.2	90	Ti-Cu
XAB	1	1	250	18	27	Ti
YAB	1	1	250	18	27	Ti

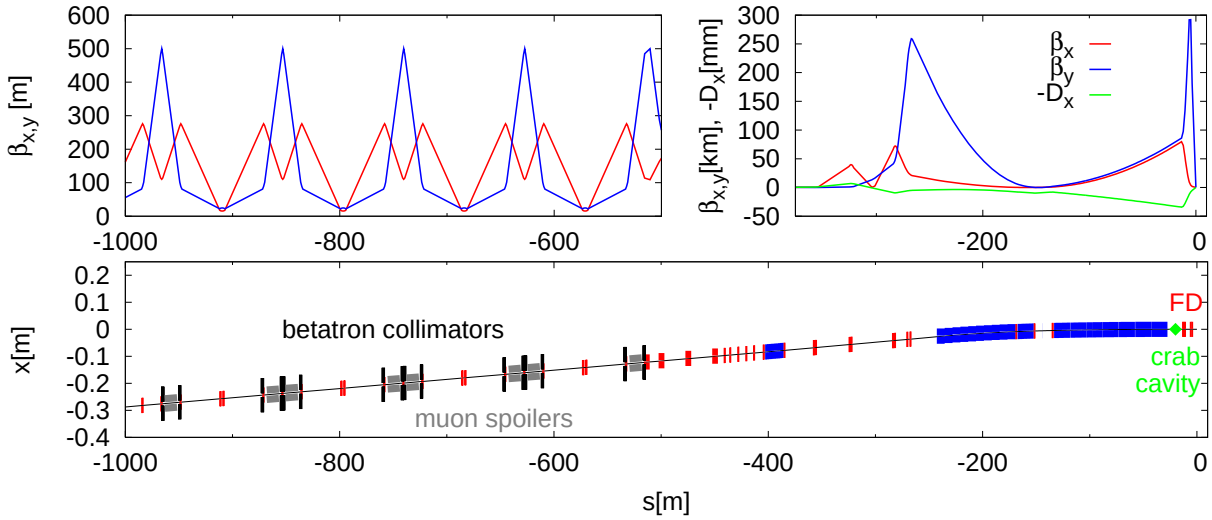

Fig. 3: Optics (top) and layout (bottom) of the CLIC betatron collimation and final focus sections.

description of the BDS spoilers and absorbers is given in Table 2.

First activation and damage studies have been carried [3] out for the energy collimation area assuming that a fraction of 10^{-6} beam particles hit the energy spoiler and that CLIC operates 200 days per year. Activation levels after one year of operation have been found acceptable for the energy spoiler and the elements downstream. The Displacement Per Atom (DPA) of the energy spoiler after one year of operation is in the 10^{-6} level, representing a negligible damage.

Particles in the beam halo produce backgrounds in the detector and must be removed in the BDS collimation system. One of the design requirements for the CLIC BDS is that no particles are lost in the last several hundred meters of beamline before the IP. Another requirement is that all synchrotron radiation passes cleanly through the IP to the extraction line. The BDS collimation must remove any particles in the beam halo which do not satisfy these criteria. These requirements define a system where the collimators have very narrow gaps and the system is designed to address the resulting machine protection, survivability and beam emittance dilution issues. The betatron collimation system has four spoiler/absorber x/y pairs located as displayed in Fig. 3. These provide collimation at each of the final doublet (FD) and IP betatron phases. All spoilers and absorbers have adjustable gaps.

There is a small probability (of the order of some 10^{-4}) that high energy secondary muons are

produced in the collimation of the halo particles which may reach the experimental cavern and detector. This was studied by detailed tracking using PLACET [5] with HTGEN [6] for the halo modeling and BDSIM [7] for the study of muon production and tracking towards the detector.

The simulated muon tracks are used as input to detector simulations. It was found, that it will be important for the detector performance that the background muon rates from the machine are kept at a low level, aiming for not more than 5 muon per bunch crossing on average, integrated for both beams and over the cross section of the detector [8].

The simulations of halo particles are based on beam-gas scattering as the primary halo source. Under favorable beam and design vacuum conditions with residual gas pressure at the 0.1-1 nTorr level both in the LINAC and the BDS, we expected that only a very small fraction, of the order of 10^{-6}-10^{-5} of the beam particles would be lost at the collimators resulting into a muon flux which would not exceed the level of 1 muon per bunch crossing.

3.5.3.4 Muon suppression

The actual fraction of halo particles in a realistic machine with imperfections is hard to predict and could be much higher than simulated by beam-gas scattering for the ideal machine. For more conservative estimates, we assume that the collimation system would be hit by a fraction of 10^{-3} of the beam particles resulting in one to two orders of magnitude higher muons rates [9] than targeted by the detector studies.

We have looked into the possibility to reduce the muon flux into the detector region using cylindrical magnetized iron shielding with an outer radius of 55 cm around the beam pipe at about 100 m downstream of the spoilers. Based on our current tracking studies using BDSIM, we expect that a factor of ten reduction of the muon flux would require a 80 m long shielding. More detailed simulations are ongoing. It will be essential to reserve the space in the drift spaces of the BDS for the muon shield as shown in Fig. 3. The actual installation of the muon shield could be done in stages, as required by the actual beam conditions.

Other muon suppression systems might also be considered during the technical phase as introducing absorbers downstream the collimators inside the beam pipe.

3.5.3.5 Final Focus

The role of the Final Focus System (FFS) is to demagnify the beam to the required size (σ_x =45 nm and σ_y =1 nm) at the IP. The FFS optics creates a large and almost parallel beam at the entrance to the Final Doublet (FD) of strong quadrupoles. Since particles of different energies have different focal points, even a relatively small energy spread of 0.1% significantly dilutes the beam size, unless adequate corrections are applied. The design of the FFS is thus mainly driven by the need to cancel the chromaticity of the FD. The CLIC FFS has a baseline local chromaticity correction [10] using sextupoles next to the final doublets. A bend upstream generates dispersion across the FD, which is required for the sextupoles and non-linear elements to cancel the chromaticity. The dispersion at the IP is zero and the angular dispersion is about 1.4 mrad, i.e. small enough that it does not significantly increase the beam divergence. Half of the total horizontal chromaticity of the final focus is generated upstream of the bend in order for the sextupoles to simultaneously cancel the chromaticity and the second-order dispersion. The horizontal and the vertical sextupoles are interleaved in this design, so they generate third-order geometric aberrations. Additional sextupoles upstream and in proper phases with the FD sextupoles partially cancel these third order aberrations. The residual higher order aberrations are further minimized with octupoles and decapoles [11]. The final focus optics is shown in Fig. 3.

3.5.3.6 Crab Cavity

With a 20 mrad crossing angle, crab cavities are required to rotate the bunches so they collide head on. They apply a z-dependent horizontal deflection to the bunch that zeroes at the center of the bunch. The

Table 3: Total luminosity and luminosity in the 1% energy peak for the various L* under consideration.

L* [m]	total luminosity $[10^{34}\text{cm}^{-2}\text{s}^{-1}]$	peak luminosity $[10^{34}\text{cm}^{-2}\text{s}^{-1}]$
3.5	6.9	2.5
4.3	6.4	2.4
6	5.0	2.1
8	4.0	1.7

crab cavity is located prior to the FD as shown in Fig. 3 but sufficiently close to be at 90° degrees phase advance from the IP.

3.5.3.7 Alternative L^*

In the nominal configuration with L*=3.5 m the last quadrupole of the FD, QD0, sits inside the detector, see Section 2.6.1 for detailed illustrations. In order to alleviate the engineering and the stabilization of this set-up it has been proposed, as a possible fallback solution, to move QD0 from the detector to the tunnel, consequently increasing L^*. A collection of FF systems with L^* values between 3.5 and 8 m has been studied for CLIC. The performance of these FFS is shown in Table 3. Both the total luminosity and the luminosity in the energy peak degrade as the L^* increases. Only the cases with L^* of 3.5 and 4.3 m meet the CLIC requirements with a 20% margin for static and dynamic imperfections. The shortest L^* that allows removing QD0 from the detector is 6 m. The FFS with L^*=6 m meets the CLIC requirements with a tight margin of 5% for the imperfections [12]. The last case with L^*=8 m does not meet the CLIC requisites.

3.5.4 Accelerator physics issues

3.5.4.1 Synchrotron radiation and the detector solenoid

Synchrotron radiation from all the BDS magnets causes a 22% luminosity loss [13]. About 10% comes from the FFS bending magnets and another 10% originates at the FD quadrupoles. The CLIC vertical IP beta function is slightly below the theoretical beta function that minimizes the Oide effect [14, 15]. These numbers do not take into account the effect of the detector solenoid as this strongly depends on the final configuration of the IR. Simulations in [16] show that the luminosity loss due to the solenoid ranges between 3% and 25%. The right adjustments of the length of the antisolenoid, the L^*, the detector solenoid field and the crossing angle should be explored to minimize this luminosity loss.

3.5.4.2 Crab Cavity effects

A proper simulation of the current crab cavity scheme has shown a 5% luminosity loss from ideal head-on collisions without crab cavities [17]. The source of this luminosity loss is identified as the aberrations caused by the crabbed beam at the sextupoles downstream of the crab cavity. Various solutions to avoid this luminosity loss have already been found as [18]: (i) compensation with an extra crab cavity [19], (ii) change the location of the crab cavity, (iii) use the opposite beam crossing scheme with opposite crab cavity voltage.

3.5.4.3 Beam pipe aperture

The aperture of the CLIC BDS beam pipe must be large enough to contain the beam ($14\sigma_x$ and $55\sigma_y$) and to avoid the effects from the resistive wall wakefield [20]. It also must be small enough to guarantee the feasibility of the BDS magnets. In [20] it is computed that a reference beam pipe radius of 8 mm

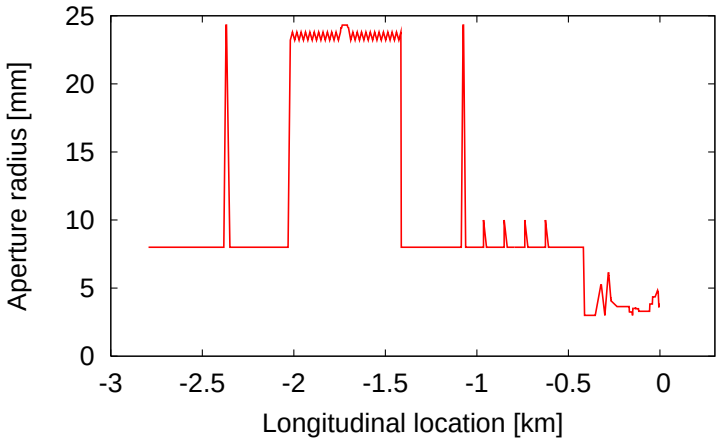

Fig. 4: Beam pipe aperture radius along the BDS.

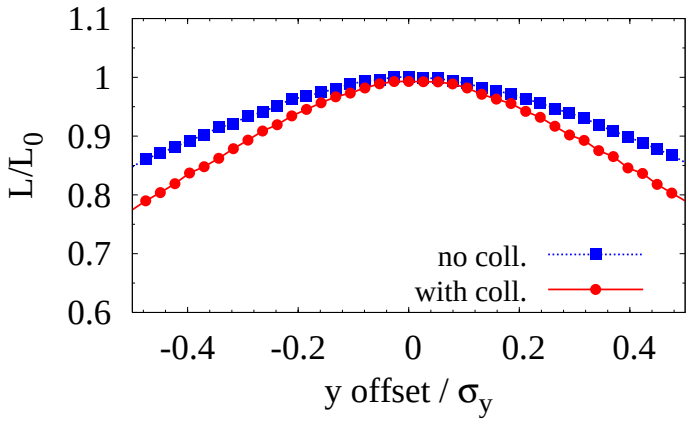

Fig. 5: Relative CLIC luminosity versus initial beam offsets for the cases with and without collimator wakefield effects.

is acceptable in terms of resistive wall effects. A larger aperture is used where the beam requires more space and a smaller aperture is used where the magnet feasibility is challenged. A round aperture is assumed all along the BDS, see Fig. 4.

3.5.4.4 Collimators wakefields

Betatron spoilers are the main source of emittance growth due to wakefields in the BDS. The effects of the collimator wakefields on the luminosity have been evaluated for the design transverse collimation apertures $15\sigma_x$ and $55\sigma_y$ and the materials as given in Table 2. Figure 5 compares the relative luminosity degradation as a function of initial vertical position offsets at the entrance of the BDS with and without collimator wakefields. In this calculation the effect of all the BDS collimators has been considered. For instance, for beam offsets of $\pm 0.4\sigma_y$, the CLIC luminosity loss was found to amount up to 20% with collimator wakefields, and up to 10% for the case with no wakefield effects.

3.5.4.5 FFS tuning

The biggest challenge faced by the BDS is the demonstration of the performance assuming realistic static and dynamic imperfections. The diagnostics and the collimation sections have demonstrated to be

robust against misalignments (prealignment of 10 μm over 500 m as discussed in 3.5.5.5). Standard orbit correction techniques, as the dispersion free steering, guarantee the beam transport without blow-up in these regions. However these techniques fail in the FFS. The CLIC FFS is a very non-linear system with a pushed β_y^* down to 0.07 mm. Many different approaches have been investigated to tune the FFS in presence of realistic misalignments. Currently the two most successful approaches follow:

- **Luminosity optimization**: Maximizes the luminosity using all the available parameters in the FFS applying the Simplex algorithm.
- **Orthogonal knobs**: Maximizes the luminosity by scanning pre-computed arrangements of sextupole displacements (knobs) which target the IP beam correlations in an orthogonal fashion.

These approaches are simulated for 100 statistical realizations of the CLIC FFS with misalignments. The final luminosity distribution and the number of iterations are shown in Fig. 6 for these two approaches in black and blue. The number of iterations corresponds to the number of luminosity measurements. A random error up to 3% has been assumed for the luminosity measurement. Neither the Simplex approach, nor the orthogonal knobs reach a satisfactory result in terms of luminosity. However being the orthogonal knobs much faster it is possible to apply it after the Simplex approach. This corresponds to the magenta curves in Fig. 6, showing 90% probabily of reaching 90% of the design luminosity and requiring a maximum of 18000 iterations. The achieved luminosity performance is close enough to the desired 90% probability of reaching 110% of the design luminosity since new approaches or extensions will further improve the final luminosity, e.g., non-linear knobs. To convert the number of iterations into time it is required to know how long a luminosity measurement will take. A conventional measurement of luminosity takes between 7 and 70 minutes [21], however faster indicators exist as different combinations of beamstrahlung signals [22] and hadronic events [23]. These studies suggest that less than 10 bunch crossings should be enough to obtain accurate signals for tuning. Therefore 18000 iterations would take about an hour, which is reasonable for tuning the BDS from scratch.

During the CLIC technical design phase special focus needs to be put in improved tuning algorithms taking into account realistic errors in all BDS elements (e.g. the solenoid and the crab cavity were excluded in this study). The e^- and e^+ BDS lines should be optimized simultaneously and more robust FFS designs could be considered.

3.5.5 Component specifications

3.5.5.1 Magnets

The CLIC BDS consists of 206 dipoles occupying 1.3 km, 70 quadrupoles occupying 190 m and 18 sextupoles over 34 m. Due to a lack of resources some BDS magnet lack an engineering design but no technical obstacle is observed a priori. Magnetic designs will be made during the next CLIC design phase.

The dipoles feature magnetic fields between 20 and 120 Gauss with a field relative precision and jitter better than 10^{-4}. The sextupolar relative field error in the dipoles at 10 mm must be below 6×10^{-4}. The baseline approach is to use normal conducting dipoles, however superconducting dipoles have the advantage of naturally shielding stray fields.

The most challenging quadrupole in the BDS is the final quadrupole QD0. Its specifications are given for the different L^* FFS options in Table 4. The technical description of QD0 is given in Section 5.10.2.1.

An antisolenoid is required to shield QD0 from the detector magnetic field [24] and to avoid the beam emittance blow-up. A more detailed view of the antisolenoid is given in Section 2.6.3.2.

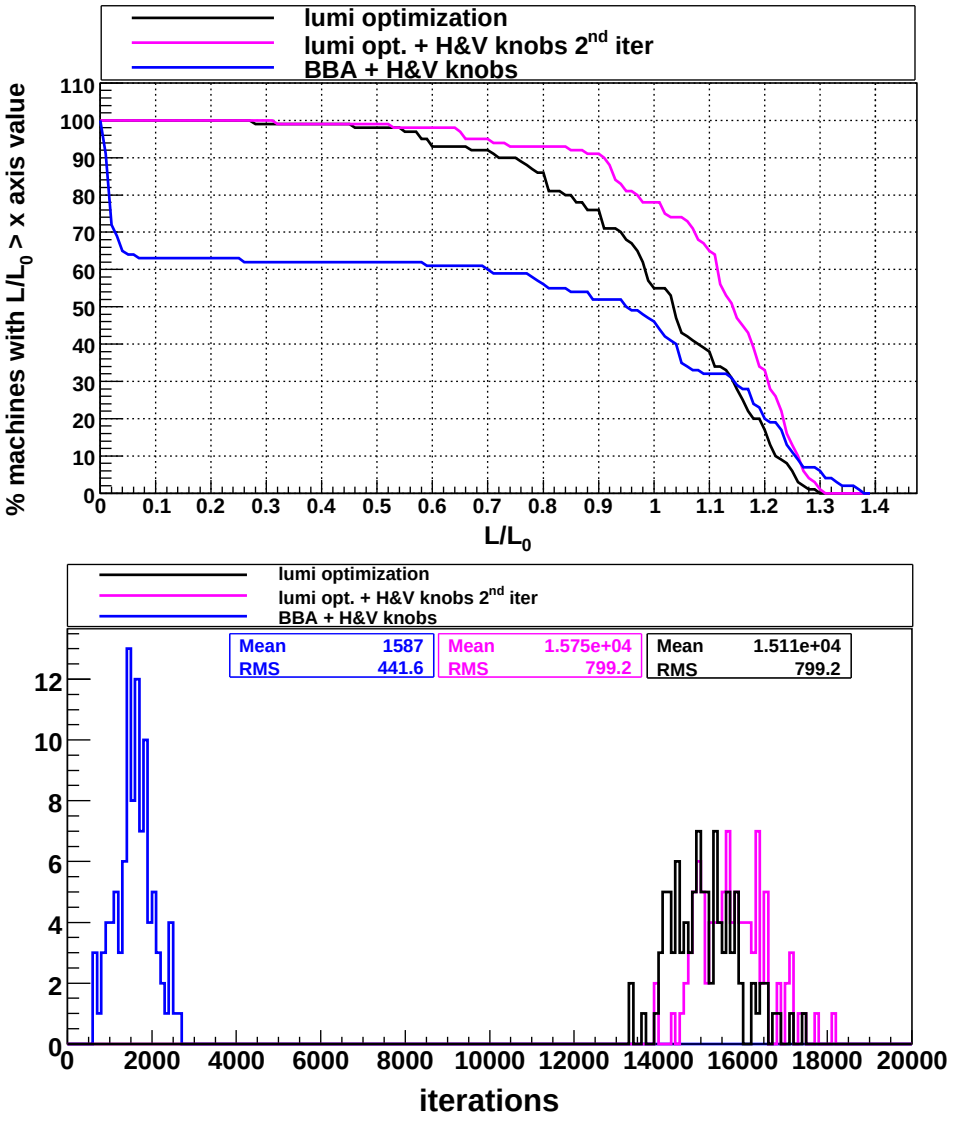

Fig. 6: Top: Luminosity performance for 100 statistical realizations of the CLIC FFS after tuning using 3 different approaches. Bottom: Required number of luminosity measurements for the 3 different approaches.

Table 4: Specifications of the FD QD0 quadrupole for the different L^* cases.

L^*	m	3.5	4.3	6.0	8.0
Gradient	T/m	575	382	200	211
Length	m	2.7	3.3	4.7	4.2
Beam aperture	mm	3.8	6.7	8	8.5
Jitter tolerance	nm	0.15	0.15	0.2	0.18
Gradient tol	10^{-6}	5	5	-	3
Octupolar error	10^{-4}@1mm	7	7	-	3
Prealignment	μm	10	10	8	2

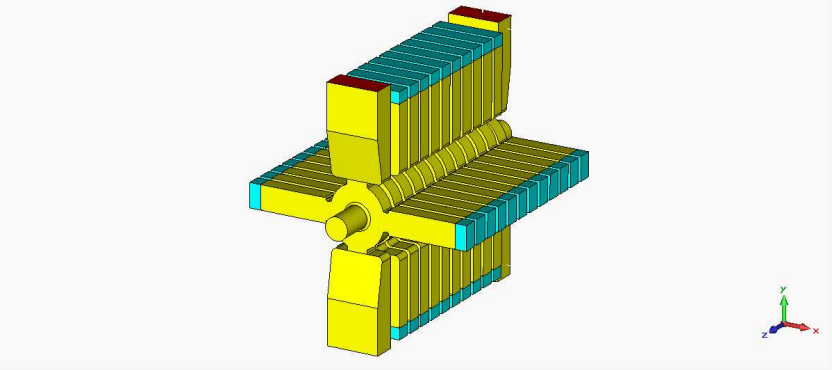

Fig. 7: 12 cell crab cavity design including wakefield dampers (length ≈300 mm).

3.5.5.2 Instrumentation

About 100 BPMs are assumed per BDS line (total of 200). Most of these BPMs need between 20 and 50 nm resolution. Few FD BPMs require 3 nm resolution in order to monitor and feedback the orbit at the FD.

Four horizontal and four vertical beam size laser wires are assumed per BDS line, see Fig. 2. The vertical laser wires should resolve a 1 μm beam with 1% resolution.

The polarization laser collides with the beam with a 10 mrad angle. It should have a wavelength of 532 nm and an IP spot size of 50 μm. This set-up guarantees a resolution of 0.1%.

Other required instrumentation as beam loss monitors, beam profile monitors, etc, will be specified during the technical design phase.

3.5.5.3 Crab cavities

The baseline crab cavities operate at 12 GHz and require a phase stability of 0.02° and an amplitude stability of 2% for a luminosity loss of 2%. Crab cavities also need strong high order mode damping. Figure 7 shows the current design of the crab cavity [25].

3.5.5.4 Vacuum

The vacuum system for the BDS can be separated into 4 main types of systems, linked by common interfaces and requirements.

There are 206 dipole magnet chambers of 24 mm internal radius and 70 quadrupole magnet chambers with 8mm inner radius where the dimensions are constrained by the surrounding magnetic elements. These are separated by drift vacuum sections where dimensions and materials can be optimized for vacuum and mechanics. Finally there are a number of special vacuum sectors containing collimators and crab cavities which will have special requirements.

The requirements from the accelerator physics side are for an average pressure better than 1 nTorr [26]. From the point of view of vacuum and surface physics, the pressure and surfaces must be designed to prevent pressure instabilities in the positron line. Additional requirements for the special vacuum sectors remain to be determined.

Preliminary pressure analysis suggests that the dipole chambers can be unbaked, with lumped ion pumps at both extremities. The small conductance of the quadrupole chambers means that a distributed pumping system along the chamber length will be required. This could use the same concept as for the main LINAC module chambers, i.e. ante-chambers with NEG pumping strips connected to the beam aperture [27].

3.5.5.5 Alignment

All elements in the CLIC BDS are assumed to be prealigned to 10 μm transversely over a distance of 500 m. The longitudinal prealignment of the elements in the FFS will be determined within $\pm$25 μm. The determination of the transverse position of each element will follow the same strategy as for the main linac (see Section 3.15). It will be performed by two different networks [28]:

- A Metrological Reference Network (MRN), consisting of overlapping wires with a length of 500 m, linked by biaxial Wire Positioning Sensors (WPS) installed and measured on a common metrological plate. The objective of this network is to propagate the precision of a few micrometers over 500 m.
- A Support Pre-alignment Network (SPN), framed by the MRN network, that associates sensors to each support to be aligned, will provide a few microns precision and accuracy over more than 10m. A third step will be required to link the support to the element to be aligned. This will be performed on a 3D Coordinate Machine Measurements (CMM), with an uncertainty of measurement of 0.3 μm + 1 ppm.

The longitudinal monitoring of the elements of Final Focus will be carried out using capacitive sensors coupled to each component. These sensors will measure with respect to targets located at the extremities of a carbon bar, independent from the components.

The solution of high precision and remote adjustment is the same as the one foreseen for the Main Beam quadrupoles (see Section 3.15.2.1), e.g. the use of eccentric cam movers. The only modification concerns the remote adjustment of the longitudinal axis in the final focus, which is not planned in the main linac. This additional adjustment will be performed by a stepper motor which will act on the blocking longitudinal point.

Bibliography

[1] http://clicr.web.cern.ch/CLICr/MainBeam/BDS/

[2] P. Schuler, "Upstream polarimeter for CLIC", CLIC08.

[3] V. Vlachoudis et al, "Energy deposition calculations on the BDS spoiler system", CLIC-Note-932.

[4] J. Resta-López, D. Angal-Kalinin, B. Dalena, J. L. Fernández-Hernando, F. Jackson, D. Schulte, A. Seryi and R. Tomás, "Status report of the baseline collimation system of CLIC. Part II.", CLIC-Note-883, 2011.

[5] D. Schulte, T.E. D'Amico, G. Guignard, N. Leros, "Simulation Package based on PLACET", PAC2001, Chicago (2001); CERN/PS 2001-028 (AE), CLIC Note 482 (2001) EUROTeV-Report-2008-076

[6] H. Burkhardt, I. Ahmed, M. Fitterer, A. Latina, L. Neukermans, and D. Schulte, "Halo and tail generation computer model and studies for linear colliders"

[7] I. Agapov, G. Blair, S. Malton, and L. Deacon, "BDSIM: A particle tracking code for accelerator beam-line simulations including particle-matter interactions," NIM-A **606** (2009), no. 3, 708 – 712.

[8] L. Linsen, "CLIC detector status" CLIC meeting June 17, 2011.

[9] H. Burkhardt, G. A. Blair, and L. Deacon, "Muon Backgrounds in CLIC", IPAC 2010

[10] P. Raimondi and A. Seryi, Phys. Rev. Lett. **86**, 3779-3782.

[11] R. Tomás, Phys. Rev. ST Accel. Beams **9**, 081001 (2006).

[12] G. Zamudio and R. Tomás, "Optimization of the CLIC 500 GeV Final Focus System and design of a new 3 TeV Final Focus System with L^*=6.0 m", CERN-OPEN-2011-035 and CLIC-Note-882, 2010.

[13] B. Dalena, D. Schulte, R. Tomás, CERN, D. Angal-Kalinin, "Solenoid and Synchrotron radiation effects in CLIC", CERN-ATS-2009-083 and CLIC-Note-786, 2009.

[14] K. Oide, Phys. Rev. Lett. **61**, 1713 - 1715 (1988).

[15] R. Tomás et al, “Summary of the BDS and MDI CLIC08 Working Group”, CLIC-Note-776.

[16] B. Dalena, D. Schulte, R. Tomás, “Impact of the experiment solenoid in the CLIC luminosity”, Proceedings of IPAC 2010.

[17] I.R.R. Shinton and R.M. Jones, “Beam dynamics effects with Crab Cavities”, 5^{th} CLIC-ILC BDS+MDI meeting.

[18] J. Barranco, E. Marín and R. Tomás, “Luminosity studies in a traveling focus scheme in the CLIC Final focus”, *to be published as CLIC Note*.

[19] A. Seryi, “Crab cavity effects on y-beam size for ILC”, January 2005 (revisited in the 3^{rd} CLIC-ILC BDS+MDI meeting).

[20] R. Mutzner et al, “Multi-Bunch effect of resistive wall in the CLIC BDS” ,CLIC-Note-818.

[21] D. Schulte, “New CLIC parameters, luminosity and background”, presented in the CLIC 08 workshop at CERN, 14-17 October 2008.

[22] P. Eliasson, M. Korostelev, D. Schulte and R. Tomás, “Luminosity tuning at the interaction point”, Proceedings of EPAC 2006, Edinburgh, Scotland.

[23] B. Dalena, J. Barranco, A. Latina, E. Marín, J. Pfingstner, D. Schulte, J. Snuverink, R. Tomás, and G. Zamudio, “BDS tuning and Luminosity Monitoring in CLIC”, CLIC-Note-931.

[24] D. Swoboda, B. Dalena and R. Tomás, “CLIC spectrometer magnet interference computation of transversal B-field on primary beam”, CERN-OPEN-2010-016 and CLIC-Note-815.

[25] A. Dexter, G. Burt, P. Ambatu, I. Shinton, R. Jones, “CLIC crab cavity specifications”, EuCARD-Milestone-M10.3.4-v7, 2010.

[26] G. Rumolo, “Parameter Specification. Vacuum System for the CLIC Beam Delivery System.”, EDMS Id: 992781 v.2.

[27] C. Garion and H. Kos "Design of the CLIC Quadrupole Vacuum Chambers", Proceedings of the PAC 2009. Vancouver, Canada.

[28] H. Mainaud Durand et al., "CLIC active pre-alignment system: proposal for CDR and program for TDR", IWAA 2010, Hamburg, Germany, 2010.